Available online at www.sciencedirect.com
SCIENCE DIRECT®
Polymer 44 (2003) 7953–7961
polymer
www.elsevier.com/locate/polymer

Effects of different kinds of clay and different vinyl acetate content on the morphology and properties of EVA/clay nanocomposites

Wei'an Zhang, Dazhu Chen, Quanbao Zhao, Yue'e Fang*

Department of Polymer Science and Engineering, University of Science and Technology of China, Hefei, Anhui 230026, People's Republic of China

Received 25 June 2003; received in revised form 7 October 2003; accepted 21 October 2003

Abstract

A series of EVA/clay nanocomposites and microcomposites have been prepared via melt-blending. Using four kinds of EVA with different vinyl acetate (VA) contents: 28, 40, 50 and 80 wt%, and four kinds of clay: three are organophilic clay (OMMT) and one unfunctionalized clay (Na-MMT), the effects of different VA content of EVA and the kinds of the clay on the morphology and properties of EVA/clay nanocomposites were systematically investigated. In previous studies, there are only two distinct nanostructures to distinguish polymer/clay nanocomposites: the intercalated and the exfoliated. But in this paper, we proposed a new nanostructure—'the wedged' to describe the dispersion degree of clay in nanocomposites, it means the sheets of clay were partly wedged by the chains of polymer. The wedged, the intercalated and the partially exfoliated structures of EVA/clay nanocomposites were characterized by X-ray diffraction (XRD) and by high-resolution transmission electron microscopy (HRTEM). The enhanced storage modulus of EVA/clay nanocomposites was characterized by dynamic mechanical thermal analysis (DMTA). The enhanced degree in the storage modulus of the OMMT on EVA/clay nanocomposites with the partially exfoliated and intercalated structure is much higher than that with wedged structure, and that with the higher VA content is higher than that with the lower. The thermal stabilities of EVA/clay nanocomposites were also studied by thermal gravimetric analysis (TGA).

Keywords: Clay; EVA; Nanocomposites

1. Introduction

Polymer/clay nanocomposites have been receiving great attention because of their unusual properties [1–4]. Compared to the conventional composites, these nanocomposites exhibit increased modulus [5–7], reduced gas permeability [8,9] and enhanced thermal stability [10,11]. In the previous studies [12], there are two distinct nanostructures identified with polymer/clay nanocomposites: the intercalated and the exfoliated. The intercalated nanocomposites are well-ordered multilayered structures where the extended polymer chain is inserted into the gallery space between parallel individual clay sheets. The exfoliated nanocomposites result from the weak interaction with the adjacent layers' gallery cations [13], where the individual layer is not parallel to each other. The formations of these structures are mainly determined by the preparation methods of polymer/clay nanocomposites and by the characters of the monomer or polymer and clay. For melt-blending, the polarity of the chains of the polymer and the basal spacing of the clay are important for the structure of the polymer/clay nanocomposites. In general, the higher the polarity of the chains of the polymer and the wider the basal spacing of the clay, the more easily polymer/clay nanocomposites with intercalated or exfoliated structure forms. Of course, the processing parameters such as processing temperature, residence time, and shearing extent can also significantly influence the morphology and properties of polymer/clay nanocomposites. Ergungor et al. [14] investigated the effect of melt temperature on the phase behavior and preferential orientation development in Nylon 6/montmorillonite nanocomposites at melt spinning temperatures ranging from 230 to 250 °C. Paul et al. [15] systematically studied the effect of melt processing conditions on the extent of exfoliation polyamide 6/clay nanocoposites, and they got the conclusion that increasing the mean residence time in the extruder generally improves

* Corresponding author. Tel.: +86-55-13601586; fax: +86-55-13606763.
E-mail address: wazhang@ustc.edu (W. Zhang).

0032-3861/$ - see front matter © 2003 Published by Elsevier Ltd.
doi:10.1016/j.polymer.2003.10.046

the delamination and dispersion. And excessive shear intensity apparently results in poorer delamiation and dispersion. Moreover, they also found that the properties of nylon 6/clay nanocomposites almost are independent of the barrel temperature (230–280 °C), but the mechanical properties of the nanocomposites are slightly improved by increasing the screw speed [16].

EVA/clay nanocomposites can be easily prepared because the EVA contains polar group, vinyl acetate (VA), which can effectively interact with clay. In the past research, Zanetti et al. [17,18] prepared EVA/clay nanocomposites by melt-blending and studied the thermal and flame-retardant properties of this material. The flame-retardant properties of EVA/clay nanocomposites were also studied by Duquesne et al [19]. They conclude that a nanostructure enables to achieve better fire performance than a micro-structure. Alexandre et al. [20] obtained EVA/montmorillonite nanocomposites with a semi-intercalated and semi-exfoliated structure also by melt-blending and found that the Yonug's modulus and the thermal stability of this nanocomposites were enhanced by montmorillonite. Li and Ha [21] studied the effects of the polar interactions between the silicate layers by using three different kinds of clay and by grafting maleic anhydride onto EVA. Jeon et al. [22] investigated the effects of a series of EVA with different content of VA (from 3 to 28 wt%) and four different types of clay on the structure of EVA/clay nanocomposites. They found the interlayer distance of MMT increased with VA content increasing. But when VA content is beyond 15 wt%, there is no further increase of interlayer distance.

In this paper, we select four types of EVA but with higher contents (from 28 to 80 wt%) and four types of clay and systematically study the effects of different VA content and different types of clay on the morphology and properties of EVA/clay nanocomposites. The relation between the morphology and properties of EVA/clay nanocomposites was further investigated by DMTA and TGA.

2. Experimental

2.1. Materials

EVA, respectively, containing 28, 40, 50 and 80 wt% VA, were supplied by Bayer Corporation., Germany. Pristine sodium montmorillonite, with a cation exchange capacity (CEC) value of about 100 mmol/100 g, was obtained from Ling An Chemicals Co. Ltd., Hangzhou, China. Octadecyltrimethyl ammonium bromide (SIAB), dioctadecyldimethyl ammonium bromide (DIAB) and tricetadecylmethyl ammonium bromide (TRIAB) were supplied by Fei Xiang Chemicals Co. Ltd., Jiangshu, China.

2.2. Preparation of OMMT

The OMMT was prepared by cationic exchange between Na-MMT and SIAB in an aqueous solution. The suspension solution containing 12.5 g Na-MMT and 4.9 g SIAB was mixed in 240 ml of distilled water. The suspension solution was stirred at 75 °C for 2 h, the exchanged MMT was filtered and washed with distilled water until no bromide ion is detected with 0.1 M $AgNO_3$ solution. Then the product was dried in vacuum oven at 60 °C for 24 h. The OMMT was obtained and then was ground with a mortar, and sieved by a Cu griddle with 280 mesh. This OMMT is denoted as SIOM. By the same preparation method, the DIOM and TRIOM can be prepared from the exchange of 12.5 g Na-MMT with 7.9 g DIAB and 9.8 g TRIAB, respectively.

2.3. Synthesis of EVA/OMMT nanocomposites

The EVA was first mixed with the OMMT in a rubber mill at 120 °C and 32 rev min^{-1} for 3 min and for another 10 min at 64 rev min^{-1}. After mixing, the samples were hot-pressed under 10 MPa to form sheets with suitable thickness for 3 min at 140 °C. The size and thickness of the sheets were dependent on the testing methods used in the present study.

2.4. Characterization of the EVA/OMMT nanocomposites

XRD patterns were obtained by using a Japanese Rigaku D/max γ_A X-ray diffractometer equipped with graphite mono-chromatized Cu K_α radiation ($\lambda = 0.154178$ nm). The scanning range was 1.5–10° with a scanning rate of 2°/min.

The microstructure of nanocomposites was imaged using a JEOL 2010 EX HRTEM. The samples for HRTEM were cut to 60 nm thick sections with a diamond knife.

The thermal gravimetric analysis (TGA) was conducted on a Perkin–Elmer Pyris 1 TGA under N_2 flow from 25 to 600 °C. The heating rate was 10 °C/min.

Dynamic mechanical analysis (DMA) was carried out on a Rheometric Scientific DMTA IV at the frequency of 1 Hz and at the heating rate of 2 °C/min from −50 to 50 °C at which the sample lost its dimensional stability.

3. Results and discussion

3.1. Characterization of the structure of EVA/clay composites

In this experiment, three clay-modifying agents were carefully chosen, in order to get the EVA/clay nanocomposites with different morphology and properties. There is a substituted long alkyl chain (C18) for SIAB, two (2C18) for DIAB and three (3C16) for TRIAB. Their structures are described in Table 1. We assumed that more the number of

Table 1
Structure of the clay-modifying agents and the basal spacing of the different kinds of clay and of the corresponding E28/clay composites

Clay	Clay modifying agents	Basal spacing (d_{001}, nm)	
		Clay	Corresponding E28/clay composites
Na-MMT		1.3296	1.32671
SIOM	$CH_3(CH_2)_{17}N^+(CH_3)_3Br^-$	1.9833	4.16441
DIOM	$(CH_3(CH_2)_{17})_2N^+(CH_3)_2Br^-$	3.61672	3.95683
TRIOM	$(CH_3(CH_2)_{15})_3N^+(CH_3)Br^-$	3.7234	4.24242

the substituted long alkyl chains of clay-modifying agents, the wider the basal spacing of the OMMT, which can make clay more organophilic and the chains of EVA more easily enter the sheets of the clay. The polarity of EVA is also of importance to the morphology and properties of the EVA/clay nanocomposites. In the previous studies, maleic anhydride is generally used to improve the polarity of the polymer [22,23]. Now, in this system, we select the EVA with higher VA content and then EVA itself can improve its polarity because VA contains a good polar group.

Fig. 1 shows the X-ray diffraction (XRD) patterns of Na-MMT and three different kinds of OMMT. Their basal spacings of the clay were calculated from the XRD peak position using the Bragg equation and were listed in Table 1. For SIOM, there is an intense peak at 4.45°, which is shifted from the broad diffraction peak of Na-MMT. This confirms that the organic quaternary ammonium salt has intercalated into the sheets of the clay and increased the basal spacing of the sheets. For the DIOM and TRIOM, the diffraction peaks become more intense, moreover, the diffraction periods are clear. Compared DIOM with TRIOM, though the number of the substituted long alkyl chains of TRIOM is one more than that of DIOM, the basal spacing of DIOM is only slightly less than that of TRIOM. Thus, OMMT with wider basal spacing basically can be obtained by using clay-modifying agent with two substituted long alkyl chains.

Fig. 2 illustrates XRD patterns of EVA/clay hybrids using different kinds of clay. E28/Na-MMT composite almost has the same basal spacing with that of Na-MMT, indicating that the chains of EVA couldn't intercalate into the sheets of Na-MMT. Thus, only E28/Na-MMT microcomposites can be formed. However, for E28/OMMT nanocomposites, there is an obvious shift of the diffraction peak towards lower angle from that of the corresponding OMMT. The weak peak of E28/SIOM nanocomposites indicates the sheets of the clay were disturbed and the structure of this nanocomposites seems partially exfoliated. But for E28/DIOM nanocomposites, its peak becomes more intense and the diffraction periods are also clearer, thus the structure of E28/DIOM nanocomposites is basically intercalated. From Table 1 and Fig. 2, we can find that the basal spacing of E28/TRIOM nanocomposites is a little wider than that of E28/SIOM nanocomposites and E28/DIOM nanocomposites. It is because TRIOM is prepared using the clay-modifying agent with three substituted long alkyl chains. The peak of E28/TRIOM nanocomposites is much weaker than that of E28/DIOM nanocomposites, which indicates this nanocomposites may be a mixture of the partially intercalated structure and partially exfoliated structure. Compared the XRD of E28/SIOM nanocomposites with that of E28/TRIOM nanocomposites, the former structure seems to be much more exfoliated. Now we proposed a question: for the same kind of EVA, why, with the number of the substituted long alkyl chain of clay-modifying agent increasing from one to three, the structure

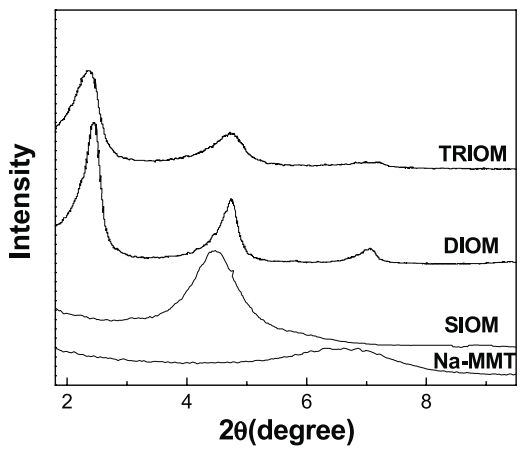

Fig. 1. XRD patterns of Na-MMT, SIOM, DIOM and TRIOM.

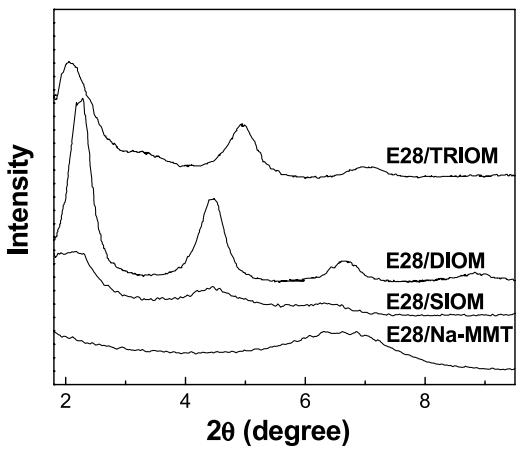

Fig. 2. XRD patterns of E28/SIOM, E28/DIOM, E28/TRIOM nanocomposites and E28/Na-MMT microcomposites.

of E28/clay nanocomposites seems to change from the partially exfoliated, then intercalated, finally to partially exfoliated? For E28/SIOM nanocomposites, its structure seems partially exfoliated. This phenomenon also appeared in the previous research [17], and the authors called the nanocomposites with this structure mixed nanocomposites and they didn't give a definite reason why this structure can be formed. We think though EVA28 contains 28 wt% VA, this amount of VA is not enough to make the chains of EVA28 and SIOM have a good interaction. When melt blending, only some of the chains of EVA were wedged into the sheets of the clay. The orderly structure of SIOM was damaged. Moreover, when the temperature becomes low, some chains move out from the sheets of the clay because the chains of EVA28 crystallize. Thus, the reason for the weak peak of the XRD patterns of E28/SIOM is that the sheets of clay were disturbed, in fact, the sheets of clay did not interact well with the chains of EVA and the clay is not well dispersed in EVA matrix. We call this nanocomposites wedged nanocomposites. This structure can be confirmed by its HRTEM (Fig. 3a). There is a big tactoids in this image, which is composed of many disordered sheets of the clay. The sheets of the clay did not interact well with the chains of EVA. When the number of the substituted long alkyl chain of clay-modifying agent increases up to two, the basal spacing of the OMMT is increased to 3.62 nm, which can supply enough space for the chains of EVA to enter. Thus the structure of E28/DIOM nanocomposites is intercalated. This intercalated structure also appeared in its HRTEM (Fig. 3b). The structure of E28/TRIOM nanocomposites is partially exfoliated because the basal spacing of TRIOM is so wide that the chains of EVA can easily enter its layers and these orderly layers are easily damaged by the mixture at 140 °C for a short time. From Fig. 3c, we can find there are many exfoliated sheets in this nanocomposites. Thus for E28/SIOM nanocomposites and E28/TRIOM nanocomposites, they all have the similar XRD patterns, only due to that they all contain the disordered sheets of the clay, but the clay is much better dispersed in E28/TRIOM nanocomposites than that in E28/SIOM nanocomposites. We draw the scheme of the four kinds of E28/clay composites in Fig. 4.

Fig. 5 shows the XRD patterns of EVA/clay nanocomposites using EVA with the different content of VA and 5% wt SIOM. For the E28/SIOM nanocomposites, the layers of the clay are not uniformly dispersed in this nanocomposites. When the amount of VA gets up to 40%, the position of the diffraction peak of E40/SIOM is almost the same with that of E28/SIOM, but the peak becomes a little more intense. But with the amount of VA further increased to 50%, the diffraction peak becomes much more intense and the periodicity of diffraction also becomes clear. This is because the sheets of the clay are still parallel to each other, though the chains of EVA have been intercalated into them. The structure of this nanocomposites is basically intercalated. Finally, when we increase the content of VA to 80%, the diffraction peak of E80/SIOM almost has the same position or intensity with that of E50/SIOM. From the above results, it can be concluded that the amount of VA is also another crucial factor for the structure of EVA/clay nanocomposites. For EVA/SIOM nanocomposites, when the amount of VA is below about 40%, only wedged nanocomposites can be formed. However, with the amount of VA increased up to above about 40%, the flexibility and polarity of the chains of EVA dramatically increase. The chain can easily crawl into the sheets of the clay to form intercalated nanocomposites. Moreover, this intercalated structure is independent of the VA content with the VA content further increasing.

3.2. Dynamic mechanical analysis of EVA/clay composites

Fig. 6a shows the storage modulus (E') of pure E28, E28/Na-MMT microcomposites and E28/SIOM nanocomposites with different SIOM content: 3 wt% (3SIOM); 5 wt% (5SIOM) and 10 wt% (10SIOM). Evidently, the E' of E28/SIOM nanocomposites increases with the amount of SIOM increased. The E' of the E28/5SIOM is 1381 MPa, which was approximately 50% higher than that of the pure EVA28. This can be interpreted as the layers of the clay interact with the chains of EVA28 and so strengthen the storage modulus of EVA28. For E28/Na-MMT microcomposites, it has a slightly lower storage modulus than that of the pure EVA28 at the temperature below their glass transition temperatures (T_gs). But, when the temperature is above their T_gs, the trend of the E' of E28/Na-MMT microcomposites is almost the same as that of pure EVA. It is because that when the temperature increases beyond the T_gs and the chains of EVA28 becomes flexible, there is almost no interaction between the clay and the chains of EVA28. The loss tangent tan δ of pure EVA28, and E28/SIOM nanocomposites and E28/Na-MMT microcomposites are shown in Fig. 6b. The peak of the tan δ curve is corresponding to the T_g. No matter for E28/SIOM nanocomposites or for E28/Na-MMT microcopmposites, their T_gs did not obviously shift towards higher temperature, compared to that of pure EVA28. Moreover, the T_g of E28/SIOM nanocomposites is also independent of the amount of the SIOM. For these wedged nanocomposites, there are only partly chains of EVA that were wedged into the sheets of the clay, and then the sheets of the clay only partly interacted with the chains of EVA. When the temperature increases, the chains are easily moved out from the sheets of the clay. Thus, the movement of the chains of the EVA28 was hardly affected by the sheets of the clay. The E' of the pure EVA80 and E80/5SIOM are presented in Fig. 7a. The E' of the E80/5SIOM is 3053 Mpa at -50 °C, which is about 62% higher than that of the pure EVA80. The enhanced degree of the SIOM on the storage modulus of the E80/SIOM is a little more than that on the E28/SIOM. The T_g of the E80/5SIOM shifts towards higher temperature, compared to that of the pure EVA80 (Fig. 7b). This is can be explained by the dispersion degree of the clay in the nanocomposites.

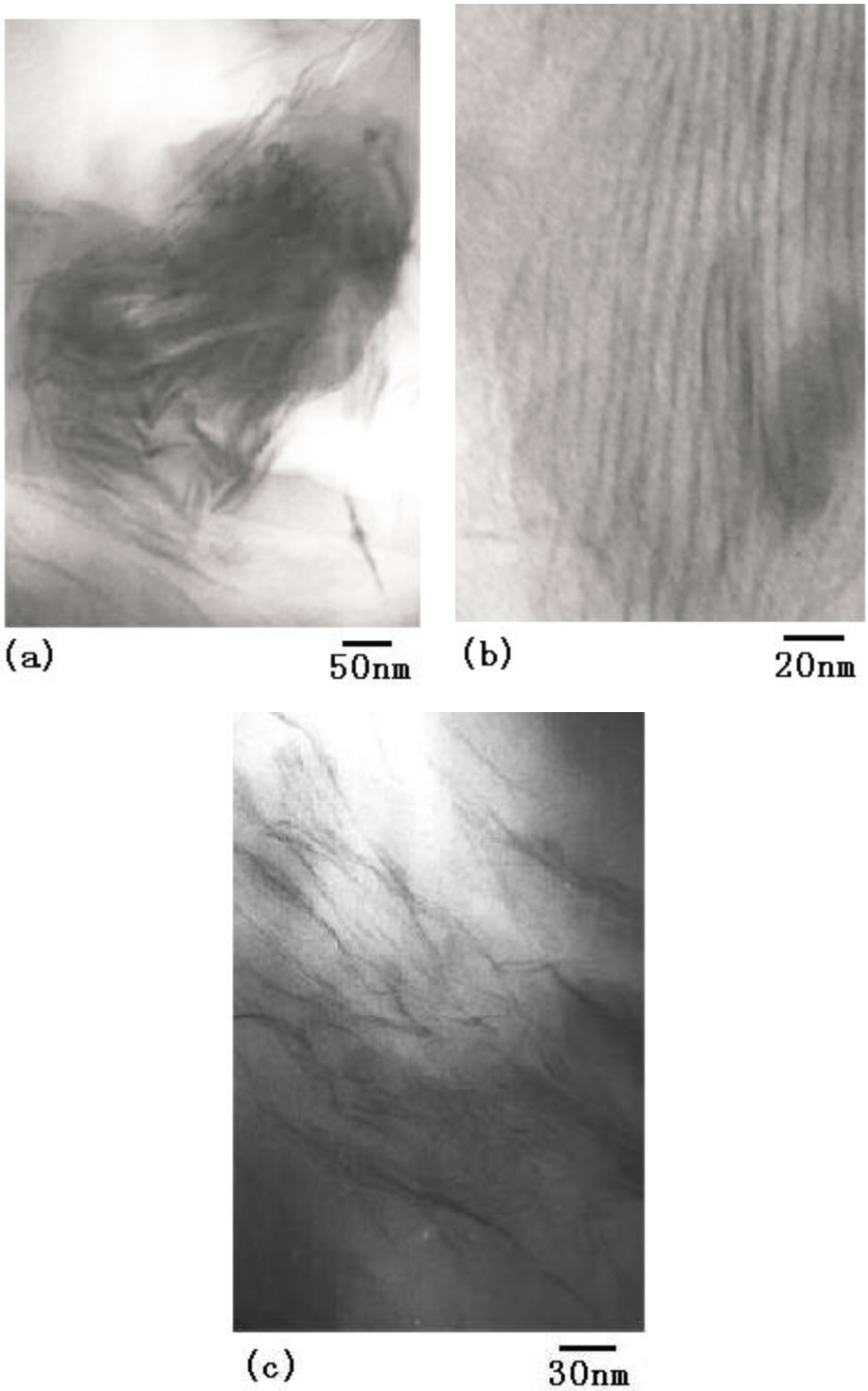

Fig. 3. HRTEM of the E28/clay nanocomposites: (a) E28/SIOM nanocomposites, (b) E28/DIOM nanocomposites and (c) E28/TRIOM nanocomposites.

Because the structure of this nanocomposites is intercalated, when the temperature increases, the movements of the chains of EVA can be checked by the sheets of the clay.

Fig. 8a shows the E' of pure E28 and E28/OMMT nanocomposites with different kinds of OMMT. We can find that the storage modulus of the E28/OMMT nanocomposites increases sequentially from E28/SIOM, E28/DIOM to E28/TRIOM nanocomposites at the temperature below their T_gs. The structure of E28/DIOM nanocomposites is intercalated, just the same with that of E80/SIOM nanocomposites. But the structure of E28/SIOM nanocomposites is wedged. The reason why the E' of the E28/DIOM nanocomposites is higher than that of E28/SIOM nanocomposites is that the sheets in this intercalated nanocomposites

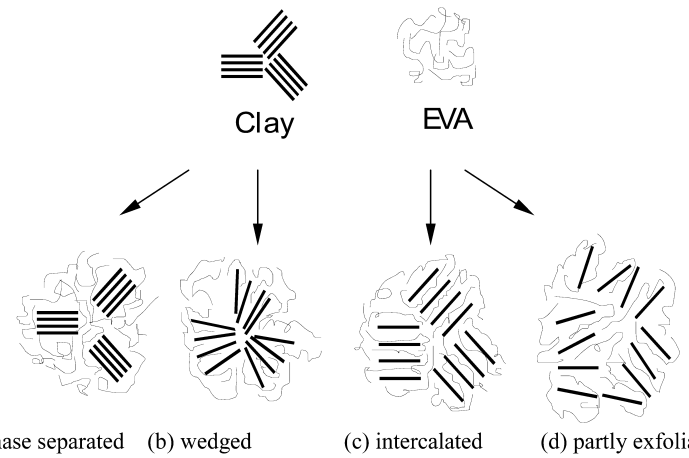

Fig. 4. Scheme of four types of EVA/clay composites with different dispersion degree of the clay sheets: (a) phase-separated microcomposites, (b) wedged nanocomposites, (c) intercalated nanocomposites and (d) partially exfoliated nanocomposites.

have a better dispersion than those in wedged nanocomposites. For the partially exfoliated E28/TRIOM nanocomposites, the sheets in this nanocomposites have much better dispersion than those in intercalated nanocomposites, thus it has much higher storage modulus.

The loss tangent tan δ of pure EVA28 and E28/OMMT nanocomposites with different kinds of the OMMT are shown in Fig. 8b. The T_g of E28/DIOM nanocomposites shifts to higher temperature compared to that of E28/SIOM nanocomposites or pure E28. Moreover, E28/TRIOM nanocomposites has a slightly higher T_g than E28/DIOM nanocomposites. This is also because the clay has a good dispersion in the intercalated E28/DIOM nanocomposites and partially exfoliated E28/TRIOM nanocomposites. In these nanocomposites, the sheets of the clay can effectively restrain the movement of the chains of EVA when the temperature increases.

3.3. Thermal gravimetric analysis of EVA/clay composites

The TGA thermograms of the pure EVA28, E28/Na-MMT microcomposites and E28/SIOM nanocomposites with different amount of SIOM in nitrogen are presented in Fig. 9. The thermal degradation temperature of EVA undergoes two stages. The first stage is attributed to the

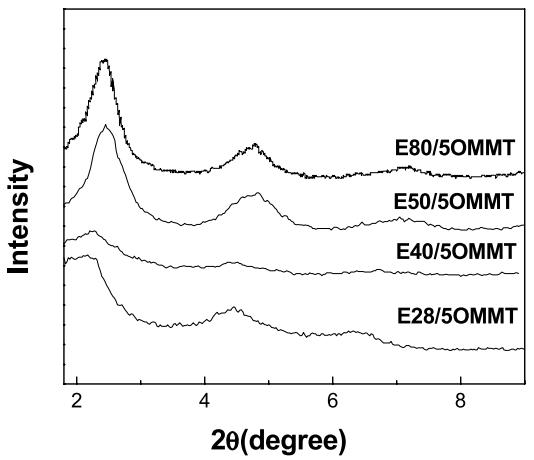

Fig. 5. XRD patterns of E28/SIOM, E40/5SIOM, E50/5SIOM and E80/5SIOM nanocomposites.

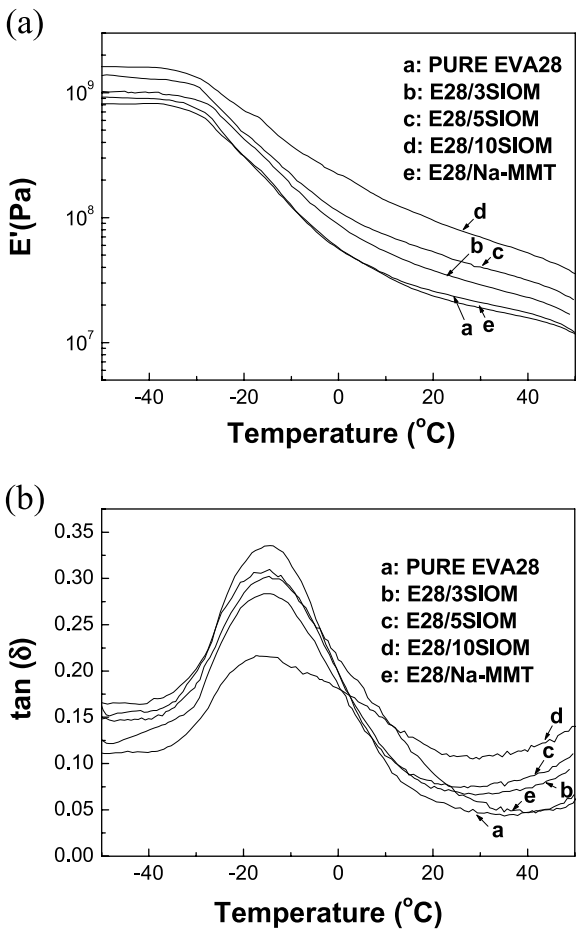

Fig. 6. (a) The trend of the storage modulus E' of PURE EVA28, E28/3SIOM, E28/5SIOM, E28/10SIOM nanocomposites and E28/Na-MMT microcomposites. (b) The tan δ vs. temperature of PURE EVA28, E28/3SIOM, E28/5SIOM, E28/10SIOM nanocomposites and E28/Na-MMT microcomposites.

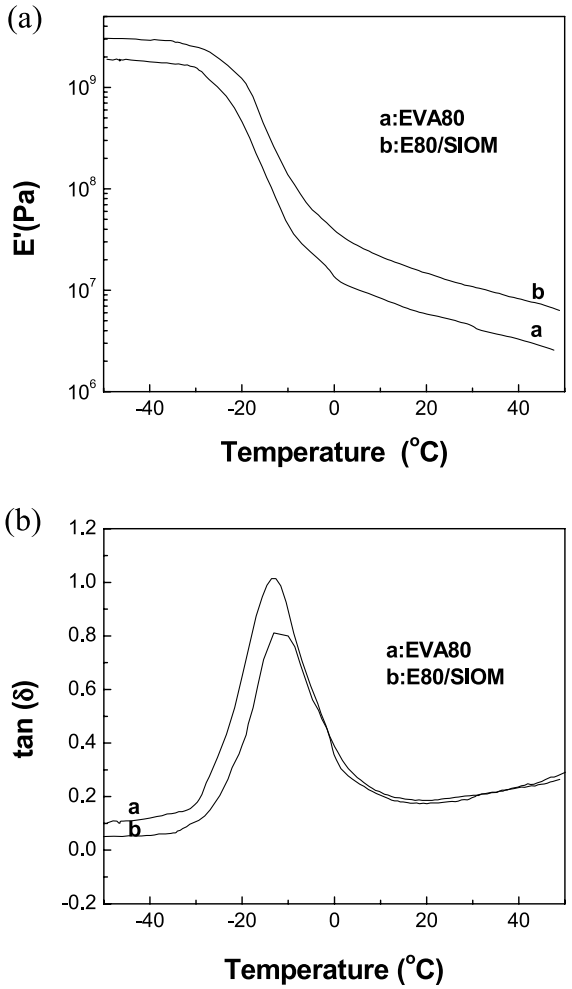

Fig. 7. (a) The trend of the storage modulus E' of PURE EVA80 and E80/SIOM nanocomposites. (b) The tan δ vs. temperature of PURE EVA80 and E80/SIOM nanocomposites.

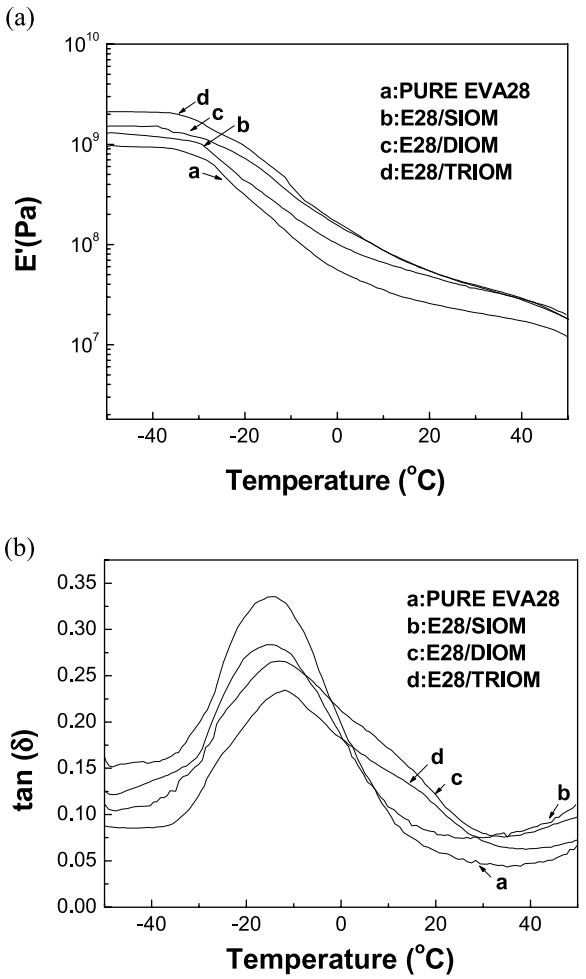

Fig. 8. (a) The trend of the storage modulus E' of PURE EVA28, E28/SIOM, E28/DIOM, E28/TRIOM nanocomposites. (b) The tan δ vs. temperature of PURE EVA28, E28/SIOM, E28/DIOM, E28/TRIOM nanocomposites.

elimination of acetic acid, which occurs at about the temperature between 310 and 405 °C. The second stage is the main-chain degradation. At the first stage, the degradation of E28/SIOM nanocomposites is much faster than that of the pure EVA, which is almost consistent with the result of Zanetti et al. [17], who used the octadecylammonium as intercalating agent to prepare OMMT. Moreover, the degradation rate increases with the content of the SIOM increased. The obvious acceleration of degradation in E28/SIOM nanocomposites may be because the previous decomposition of octadecyltrimethylammonium and its degradation product can induce the decomposition of the acetic acid. However, for E28/Na-MMT microcomposites, it has a bit better thermal stability than pure EVA28. When the temperature is about between 405 and 460 °C, E28/SIOM nanocomposites almost keep the level stage. But the pure EVA28 and E28/Na-MMT microcomposites are still losing weight at a low speed. At the temperature beyond about 460 °C, we find E28/SIOM nanocomposites have a higher thermal decomposition temperature, because MMT

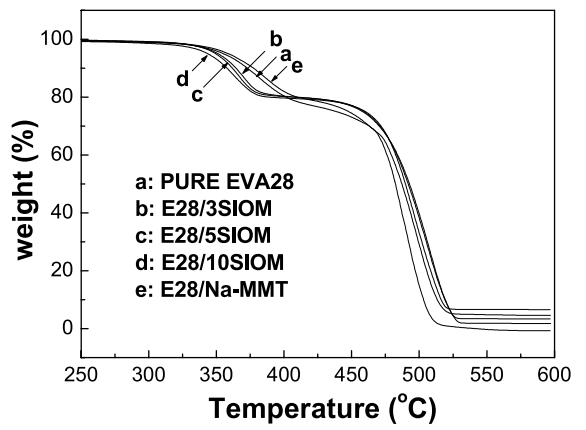

Fig. 9. TGA thermograms of PURE EVA28, E28/3SIOM, E28/5SIOM, E28/10SIOM nanocomposites and E28/Na-MMT microcomposites in nitrogen.

has an excellent barrier property and prevents against the permeation of atmospherical air and assists in the formation of char after thermal decomposition.

For E28/DIOM nanocomposites and E28/TRIOM nanocomposites, their thermal degradation rate in nitrogen is slightly faster than that of pure E28 at the first stage (Fig. 10 and Table 2), and the OMMT can also enhance the thermal stability of the main chains of EVA at the second stage. For all the E28/OMMT nanocomposites, they all have a faster degradation rate due to the beforehand degradation of clay-modifying agents, which can accelerate the decomposition of the acetic acid. But for the wedged E28/SIOM nanocomposites, the clay is not well dispersed. When the temperature increases, the sheets of clay cannot effectively check the decomposition of the acetic acid. On the contrary, the decomposition of the acetic acid is accelerated. But for E28/DIOM nanocomposites and E28/TRIOM nanocomposites, they all slightly accelerate the decomposition of the acetic acid. It is because the clay has a good dispersion in these nanocomposites and the degradation perhaps only occurs at the surface of the nanocomposites to form the char between the sheets of the clay, which can effectively prevent clay-modifying agents and the acetic acid from further degradation. When the temperature further increases to beyond about 460 °C, the acetic acid and clay-modifying agents have completely decomposed and the degradation of the main chain begins. We find the clay can effectively improve the thermal degradation temperature of the main chain.

The TGA thermograms of the pure EVA28, E28/Na-MMT microcomposites and E28/SIOM nanocomposites with different amount of SIOM in air are presented in Fig. 11 and Table 2. Compared to the degradation in nitrogen atmosphere, their thermal degradations still undergo two stages and do not obviously shift to low temperature. But the thermal degradation of E28/SIOM nanocomposites is obviously different from that in nitrogen. The first degradation stage, the elimination of acetic acid, is effectively enhanced by the SIOM, moreover, the degradation rate decreases with the amount of the SIOM increasing. But for the second degradation stage, the main degradation is restrained by SIOM, and this result is also the same with that of Zanetti et al [17]. At the 30% weight loss, the degradation temperature of E28/10SIOM nanocomposites has about 60 °C increase, compared with that of pure EVA28. Moreover, for E28/Na-MMT microcomposites, it also has obviously degradation temperature increase. But its enhanced degree is not intense as that of E28/SIOM nanocomposites, because the clay sheets are not well dispersed in E28/Na-MMT microcomposites.

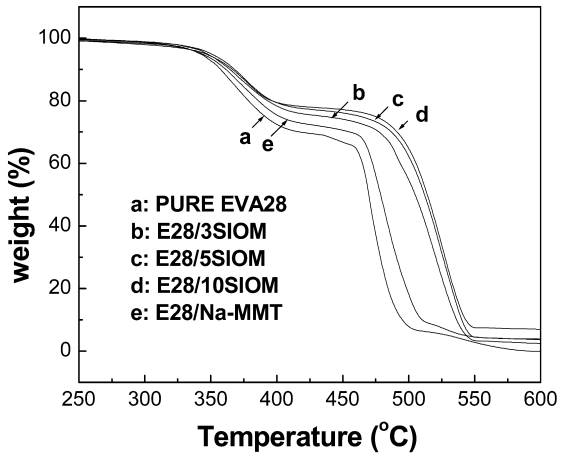

Fig. 11. TGA thermograms of PURE EVA28, E28/3SIOM, E28/5SIOM, E28/10SIOM nanocomposites and E28/Na-MMT microcomposites in air.

For E28/DIOM nanocomposites and E28/TRIOM nanocomposites, their thermal-oxidation degradations are similar with that of E28/SIOM nanocomposites (Fig. 12 and Table 2), which shows the OMMT enhance the thermal stability of EVA. But their enhanced degrees are slightly lower than that of E28/SIOM nanocomposites, even if the clay sheets have a good dispersion in these nanocomposites. This may be because the previous thermal-oxidation decomposition of

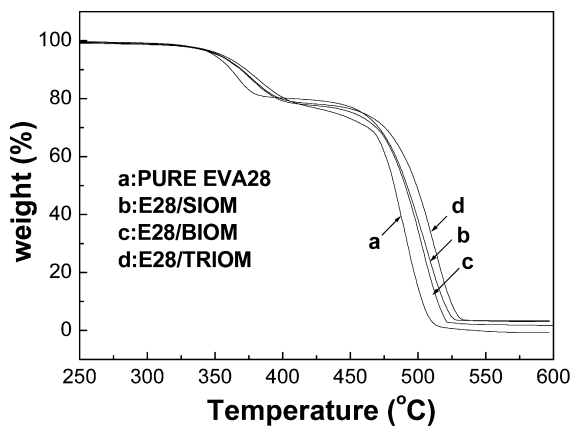

Fig. 10. TGA thermograms of PURE EVA28, E28/SIOM, E28/DIOM and E28/TRIOM nanocomposites in nitrogen.

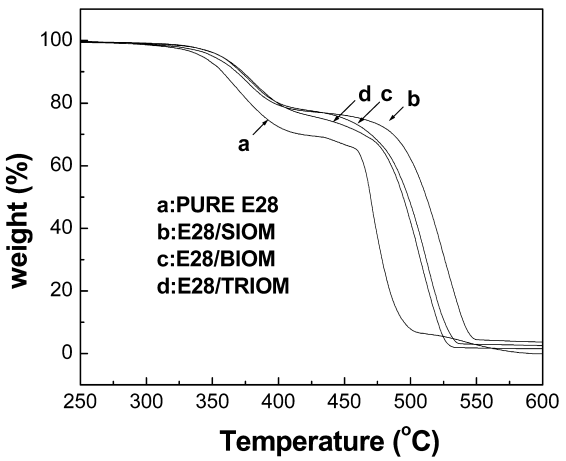

Fig. 12. TGA thermograms of PURE EVA28, E28/SIOM, E28/DIOM and E28/TRIOM nanocomposites in air.

Table 2
Properties of pure EVA and EVA/clay composites

Sample	E' (10^9 Pa)	T_g (°C)	T (°C) for 10 wt% loss in nitrogen	T (°C) for 30 wt% loss in nitrogen	T (°C) for 10 wt% l oss in air	T (°C) for 30 wt% loss in air
PURE EVA28	0.92175	−14.8	373.136	463.262	357.434	417.091
E28/Na-MMT	0.81605	−14.8	377.408	463.264	361.182	455.051
E28/3SIOM	1.02014	−14.8	362.449	470.55	364.443	477.475
E28/5SIOM	1.32962	−14.8	362.059	470.988	367.841	486.607
E28/10SIOM	1.5961	−14.8	357.988	471.888	366.364	490.834
E28/DIOM	1.5208	−13.1	369.197	469.152	371.356	469.921
E28/TRIOM	2.10804	−11.9	369.688	475.564	372.827	464.075

the intercalating agents in E28/DIOM nanocomposites and E28/TRIOM nanocomposites and their degradation products can accelerate the decomposition of the chains of EVA.

4. Conclusion

EVA/clay nanocomposites were synthesized by using organophilic clays via melt blending. For E28/SIOM nanocomposites, the clay is not well dispersed in the nanocomposites, and only wedged nanocomposites can be formed. With the amount of SIOM increasing, the E' of E28/SIOM nanocomposites increases and its T_g hardly changes, but the degradation of acetic acid increases. With the VA content and the basic spacing of the OMMT increasing, the chains of the EVA are more easily intercalated into sheets of the clays to form intercalated or partially exfoliated nanocomposites. For EVA28/clay nanocomposites, the intercalated and the partially exfoliated nanocomposites both have a more obvious increase of their mechanical and thermal properties than that of wedged nanocomposites. Moreover, partially exfoliated nanocomposites has more obvious improvement of thermal and mechanical properties than intercalated nanocomposites. Therefore the polarity of the EVA and the basal spacing of OMMT are of importance to the morphology and properties of EVA/clay nanocomposites.

References

[1] Usuki A, Kawasumi M, Kojima Y, Okada A, Kurauchi T, Kamigaito O. J Mater Res 1993;8:1174.
[2] Giannelis EP. Adv Mater 1996;8:29.
[3] Biswas M, Ray SS. Adv Polym Sci 2001;155:167.
[4] Wang Z, Pinnavaia TJ. Chem Mater 1998;10:3769.
[5] Maiti P, Yamada K, Okamoto M, Ueda K, Okamoto K. Chem Mater 2002;14:4654.
[6] Yao KJ, Song M, Hourston DJ, Luo DZ. Polymer 2002;43:1017.
[7] Kawasumi M, Hasegawa N, Kato M, Usuki A, Okada A. Macromolecules 1997;30:6333.
[8] Chang JH, Park KM, Cho DH, Yang HS, Ihn K. J Polym Engng Sci 2001;41:1514.
[9] Usuki A, Tukigase A, Kato M. Polymer 2002;43:2185.
[10] Zhu J, Uhl FM, Morgan AB, Wilkie CA. Chem Mater 2001;13:4649.
[11] Gilman JW. Appl Clay Sci 1999;15:31.
[12] Alexandre M, Dubois P. Mat Sci Engng R 2000;28:1.
[13] Lan T, Pinnavaia TJ. Chem Mater 1994;6:2216.
[14] Ergungor Z, Cakmak M, Batur C. Macromol Symp 2002;185:259.
[15] Dennis HR, Hunter DL, Chang D, Kim S, White JL, Cho JW, Paul DR. Polymer 2001;42:9513.
[16] Cho JW, Paul DR. Polymer 2001;42:1083.
[17] Zanetti M, Camino G, Thomann R, Mullhaupt R. Polymer 2001;42:4501.
[18] Zanetti M, Kashiwagi T, Falqui L, Camino G. Chem Mater 2002;14:881.
[19] Duquesne S, Jama C, Le Bras M, Delobel R, Recourt P, Gloaguen JM. Compos Sci Technol 2003;63:1141.
[20] Alexandre M, Beyer G, Henrist C, Cloots R, Rulmont A, Jerome R, Dubois P. Macromol Rapid Commun 2001;22:643.
[21] Li XC, Ha CS. J Appl Polym Sci 2003;87:1901.
[22] Jeon CH, Ryu SH, Chang YW. Polym Int 2003;52:153.
[23] Nam PH, Maiti P, Okamoto M, Kotaka T, Hasegawa N, Usuki A. Polymer 2001;42:9633.